THE JOURNAL OF PHYSICAL CHEMISTRY C

Article

pubs.acs.org/JPCC

Probing the Perturbation of Lecithin Bilayers by Unmodified C_{60} Fullerenes Using Experimental Methods and Computational Simulations

Nikolaos Bouropoulos,[*,†,‡] Orestis L. Katsamenis,[†,§] Paul A. Cox,[∥] Simon Norman,[∥] Paraskevi Kallinteri,[⊥,▽] Marco E. Favretto,[#] Spyros N. Yannopoulos,[‡] Aristides Bakandritsos,[†] and Dimitrios G. Fatouros[∥,○]

[†]Department of Materials Science, University of Patras, 26504 Rio, Patras, Greece

[‡]Foundation for Research and Technology, Hellas-Institute of Chemical Engineering and High Temperature Chemical Processes - FORTH/ICE-HT, P.O. Box 1414, GR-26504 Patras, Greece

[§]Bioengineering Research Group, University of Southampton, Southampton, SO17 1BJ, United Kingdom

[∥]School of Pharmacy and Biomedical Sciences, University of Portsmouth, St. Michael's Building, White Swan Road, Portsmouth PO1 2DT, United Kingdom

[⊥]Medway School of Pharmacy, Universities of Kent/Greenwich, Central Avenue, Chatham Maritime, ME4 4TB, Kent, United Kingdom

[#]Department of Biochemistry Nijmegen Centre for Molecular Life Sciences, Radboud University Nijmegen Medical Centre, Nijmegen, NL-6500 HB, The Netherlands

ABSTRACT: In this study, we aimed to use physicochemical and theoretical tools to understand fundamental problems of the interaction between lipid bilayers (Egg-PC liposomes) and unmodified C_{60} fullerenes. The morphology, the size, and the electrokinetic properties of plain and C_{60}-loaded liposomes were investigated by means of atomic force microscopy, dynamic light scattering, and ζ-potential studies, respectively. The incorporation of C_{60} molecules into the liposomes increases their size; however, there was no effect on their electrokinetic properties. Visualization studies revealed that the presence of C_{60} in the membranes induced distortion in vesicle morphology, resulting in nonspherical vesicles. To elucidate further the impact of C_{60} molecules on lipid bilayers, we assessed their miscibility by fluorescence spectroscopy measurements. Fluorescence measurements showed that the presence of C_{60} in liposomes causes a pronounced effect on the Nile red emission spectrum due to alterations to the packing of the lipid membrane. The release of vesicle-encapsulated calcein was used as a measure of the integrity of the liposomes. Plain liposomes were found to be more stable compared with C_{60}-loaded (PC) liposomes, suggesting that C_{60} ruptures the liposome membrane. Toxicity studies of C_{60} in liposomes were carried out on cultured cells [rodent fibroblasts (3T3)] to assess further their toxicity. The results suggest that fullerene cytotoxic effect was reduced significantly after its incorporation into the liposomal bilayer after 24 h of incubation with the rodent fibroblasts (3T3). Finally, energy minimization studies were employed to underpin the experimental observations. The theoretical calculations show that low concentration of fullerene molecules present in the membrane had no effect on the membrane integrity; however, at high concentrations of fullerenes significant enlargement of the surface area is observed, supporting the experimental findings.

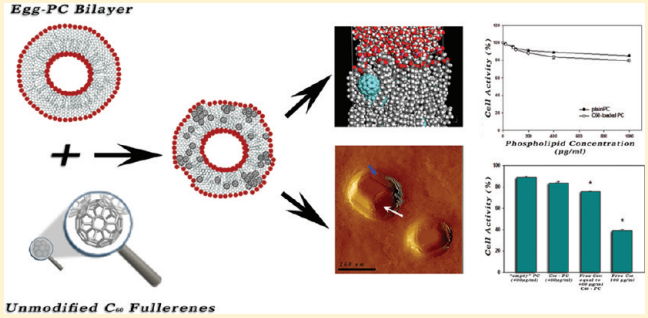

INTRODUCTION

Fullerenes have been used in several biological processes as antioxidants in cosmetic products,[1] drug carriers,[2] or molecular imaging probes.[3] They have the ability to function as a free radical sponge and quench various free radicals more efficiently than conventional antioxidants[4] and to migrate through the entire body, including the blood-brain barrier, without adsorbing serum proteins.[5] However their poor water solubility has severely limited their use in applications. An approach to overcome this obstacle is the use of various amphiphilic molecules[6] including phospholipids.[7] Moreover, the use of liposomes might reduce the reported toxicity of these materials.[8,9] Liposomes have been used widely as drug delivery systems. The main advantages of liposomes as a drug delivery system are the following: (i) they have a very versatile structure that can be easily tailored to bear the properties needed for each specific

Received: July 1, 2011
Revised: January 16, 2012
Published: January 18, 2012

application, (ii) they can accommodate any type of drug molecules either in their aqueous compartments (hydrophilic drugs) or in their bilayers (lipophilic drugs) or both (ampliplilic drugs), and (iii) they are nontoxic, nonimmunogenic and fully biodegradable.[10] Studies of the interaction of lipid membranes (liposomes) with fullerenes might provide insightful information into phenomena like membrane fusion, channel opening, and structural transitions that occur upon lipid−fullerene interactions. Several studies have combined fullerenes with lipid bilayers using both experimental[11−18] and theoretical approaches.[19−22] However, little is known on the effect of fullerenes or fullerene derivatives on the miscibility of the liposomal membrane using experimental approaches[23,24] and consequently the stability of fullerene-loaded liposomes over time. In an attempt to shed light onto such interactions, we investigated the effect of C_{60} on the membrane integrity of PC liposomes combining experimental and theoretical tools.

MATERIALS AND METHODS

Materials. Unmodified C_{60} fullerenes, calcein, Nile Red (NR), and Triton X-100 were obtained from Sigma-Aldrich (U.K.). Thiazolyl blue tetrazolium, Sephadex G-50 and buffer salts were purchased from Sigma-Aldrich. The components used for cell culture were from Gibco, U.K. L-α-Phosphatidylcholine (egg-PC) was purchased from Avanti Lipids (Alabaster, AL). Organic solvents were obtained from Fischer Scientific U.K. All solutions were prepared by Millipore water (conductivity <0.5 $\mu S \cdot cm^{-1}$).

Preparation of the C_{60} Solution. A stock solution of C_{60} in $CHCl_3$ with a final concentration of 0.2 mg/mL was prepared by adding 2 mg of C_{60} to 10 mL of $CHCl_3$. The dispersion was subjected to sonication in a bath sonicator (Branson, Danbury, CT) for 2 h until a brownish solution was obtained. The solution remained stagnant for 2 weeks, and the amount of the solubilized C_{60} was quantified by UV−vis spectroscopy (Lambda 35; Perkin-Elmer, USA).

Liposome Preparation. Liposomes consisting of L-α-phosphatidylcholine were prepared by the thin film method. In brief, 6.5 μmol of PC and 0.15 μmol of C_{60} (molar ratio of C_{60}/PC: 2.3%) were dissolved in $CHCl_3$ in a spherical flask, and the organic solvent was removed in a rotary evaporator. The film was rehydrated with 1 mL of PBS pH 7.4 and was sonicated for 60 min in a bath sonicator. The amount of C_{60} encapsulated in the PC liposomes was determined by measuring the residual free C_{60} as follows: The C_{60}-containing liposome suspension was loaded in a Sephadex G-50 (1 × 35 cm) column equilibrated with PBS at pH 7.4. Presaturation of the column was performed with the lipid. The final lipid concentration was measured by using a phospholipid colorimetric assay.[25] The nonencapsulated material that remained on the top of the column[7] was collected and mixed with 5 mL of $CHCl_3$ to extract the C_{60} and was further quantified by UV-spectroscopy.

Dynamic Light Scattering and ζ-Potential Studies. The particle size was measured by dynamic light scattering (DLS). Normalized intensity−time correlation functions $g^{(2)}(q,t) = \langle I(q,t)I(q,0)\rangle/\langle I(q,0)\rangle^2$, were measured over a broad time scale (from 10^{-7} to 10^4 s) using a full multiple tau digital correlator (ALV-5000/FAST) with 280 channels spaced quasi-logarithmically. The scattering wavevector $q = 4\pi n \sin(\theta/2)/\lambda_o$ depends on the scattering angle θ ($\theta = 90^o$ was used in the present work), the laser wavelength λ_o, and the refractive index of the medium n. The 671 nm line from a diode pumped solid-state laser was used in the present study operating at a power of <5 mW. The scattered light was collected by a single-mode optical fiber, which provided a high coherence factor (~0.95) and transferred to an avalanche photodetector and then to the digital correlator for analysis. Accumulation times were on the order of a few seconds because of the strong scattered intensity from the depressions. Several time correlation functions were recorded for each dispersion to check the reproducibility of the results. Under the assumption of homodyne scattering conditions, which are easily fulfilled in dilute suspensions as in the present case, the desired normalized electric-field time autocorrelation function

$$g^{(1)}(q, t) = \langle E(q, t)E^*(q, 0)\rangle/\langle E(q, 0)\rangle^2 \quad (1)$$

is related to the experimentally recorded intensity autocorrelation function $g^{(2)}(q,t)^2$ through the Siegert relation[26]

$$g^{(2)}(q, t) = B[1 + f^*|g^{(1)}(q, t)|^2] \quad (2)$$

where B describes the long delay time behavior of $g^{(2)}(q,t)$ and f^* represents an instrumental factor obtained experimentally from measurements of a dilute polystyrene/toluene solution. In our case, the optical fiber collection results in $f^* \approx 0.95$.

The electric-field time correlation function $g^{(1)}(t)$ (for simplicity we drop the q dependence in the following) was analyzed as a weighted sum of independent exponential contributions, that is

$$g^{(1)}(t) = \int L(\tau)\exp(-t/\tau)\,d\tau = \int L(\ln\tau)\exp(-t/\tau)\,d\ln\tau \quad (3)$$

where the second equality is the logarithmic representation of the relaxation times. The distribution of relaxation times $L(\ln\tau) = \tau L(\tau)$ was obtained by the inverse Laplace transformation (ILT) of $g^{(1)}(q,t)$ using the CONTIN algorithm.[27] The apparent hydrodynamic radii of the suspended "particles" were determined using the Stokes−Einstein relation

$$R_h = \frac{k_B T}{6\pi n D} \quad (4)$$

where k_B is the Boltzmann constant, η is the viscosity of the solvent, and D the particle self-diffusion coefficient. The latter is determined by $D = 1/\tau q^2$, where τ is the relaxation time of $g^{(1)}(q,t)$. Electrophoretic measurements for the determination of ζ-potential values of the suspensions were performed in a Malvern Instrument Nano ZetaSizer (U.K.) equipped with a 4 mW He−Ne laser, operating at a wavelength of 633 nm and having an avalanche photodiode as a detector. Data were acquired with laser Doppler velocimetry and the phase analysis light scattering (PALS) mode after equilibration at 25 °C.

Fluorescence Spectroscopy. Fluorescence measurements were performed at 25 °C on a fluorescence spectrophotometer (F2500; Hitachi, Japan) using a quartz cell with a light path of 10 mm. Specifically, 1.5 mL from the suspensions was placed in a 1 cm quartz cuvette and emission spectra were recorded at 90° during excitation at 448 nm. For this purpose, a hydrophobic dye, NR, was added in the liposomes at a concentration of 7.5 μM.

Visualization Studies. Surface topography images of plain- and C_{60}-loaded liposomes were obtained by means of atomic force microscopy (AFM). A droplet of the liposomal suspension was placed onto freshly cleaned mica and left for several minutes to allow vesicles to adsorb onto the mica. During this time, the extra water surrounding the adsorbed vesicles was evaporated, leaving behind a thin water film, which covered the sample. Following this, the sample was imaged in tapping mode (in air) with the constant force method.

(The force between the sample surface and the AFM tip was kept constant by a feedback system while the surface beneath the tip was scanned.) The samples were scanned with the minimum possible image force to minimize the potential deformation of the vesicle due to tip compression with the aid of MultiMode Scanning Probe Microscopy (Veeco) using a Nanoscope IIIa controller and a 120 μm × 120 μm magnet-free scanner (model AS-130VMF) developed by Digital Instruments with vertical range of 5 μm and a z-axis resolution of 0.05 nm. The scan rate was 1 Hz. The cantilever's spring constant was 10 N/m. The shape of the silicon nitride tips was square pyramidal with radius of curvature ~10 nm and half angle ~15°. The images were processed with a linear plane fit to remove any sample tilt on them. Final contrast/lighting adjustments of all images were performed on Adobe Photoshop CS4.

Membrane Integrity Studies. The release of vesicle-encapsulated calcein (100 mM) was determined with the separation of free and liposomal dye, as reported elsewhere.[28]

The membrane integrity of liposomes after incubation in buffer at 37 °C was evaluated by calculating the percentage of calcein latency (%) of liposome-encapsulated calcein, as previously described.[29] In brief, 10 μL was withdrawn from each incubation tube and diluted with 4 mL of PBS, pH 7.40. The fluorescence intensity of this sample was measured (Varian Cary Eclipse U.S., emission 490 nm, excitation 520 nm) before and after the addition of Triton X-100 at a final concentration of 1% (v/v). The percentage of calcein latency (%) was calculated using the following equation

$$\%\text{latency} = \frac{F_T - F_I}{F_T} \times 100 \quad (5)$$

where F_I and F_T are the calcein fluorescence of the sample in the absence and presence of 1% Triton X-100 (final concentration), respectively. These values, obtained after mixing the samples with Triton X-100, were corrected accordingly for dilution.

Proliferative Studies. Viability of 3T3 cells was evaluated using the thiazolyl blue tetrazolium bromide (MTT) assay, which is associated with cell mitochondrial activity. The assay is based on the ability of viable cells to convert MTT solution to blue formazan crystals in their mitochondria.[30] Cells were cultured in Dulbecco's modified Eagle's medium (DMEM) supplemented with 10% fetal calf serum (FCS) at 37 °C in a 5% CO_2 incubator. 3T3 cells were seeded at a concentration of 5×10^4 cells/mL/well in 24-well plates and left for 24 h to adhere on the plates. Then, they were incubated with either plain liposomes or free fullerenes or fullerene-loaded liposomes at increasing concentrations for 1 day. The cells in the first three wells were incubated in the absence of any of the formulations. DMSO (0.5 mL/well) was used as positive control for cell death. After 24 h of incubation, 100 μL of MTT solution (concentration 5 mg/mL) was added to the wells and incubated for 2 h at 37 °C. The blue formazan salts were dissolved in 100 μL of acidified isopropanol (0.33 μL HCl in 100 mL of isopropanol), which was transferred to 96-well plates, and the absorbance was read on a microplate reader (Bio-Tec Instruments, U.S.) at wavelength of 490 nm. Viability of the cells was calculated by comparing the number of viable cells in the formulation-treated wells to the nonformulation treated cells.

Molecular Simulation Studies. Energy minimization calculations were used to investigate the mode of insertion of the C_{60} to the lipid bilayers. A simulated annealing protocol was used prior to energy minimization to help ensure that a global minimum energy was obtained. Simulations were carried out using the CVFF forcefield as implemented in the Materials Studio (v4.1, Accelrys Software, San Diego, CA),[31] The CVFF forcefield has been widely used to investigate successfully the properties of phospholipid membranes.[32−38] One advantage of using this forcefield in this particular study is that a consistent set of potentials could be used for the lipid bilayer and the C_{60} molecules, with the $(C = 2)$ parameter used for the carbon atoms within the fullerene. The simulation box used for the bilayer was constructed using two 4 × 4 arrays of PC molecules. Initially, the dimensions of the box were 35 Å × 30 Å × 120 Å, although the dimensions of the box were allowed to vary throughout both the simulated annealing and the energy minimization part of the simulation. Calculations were performed in parallel on a 16 processor Linux cluster. Periodic boundary conditions were applied to simulate an infinite array, with Ewald summation used ensure appropriate treatment of long-range electrostatic interactions. Water molecules were added above and below the bilayer using the Soak algorithm. In total, 5382 water molecules were included. The simulated annealing routine involved slowly reducing the simulation temperature of the system through temperatures of 750, 500, 300, and 100 K using molecular dynamics (MD) with a simulation time of 10 ps at each temperature. Finally, energy minimization using a combination of the steepest descents and conjugate gradients methods was performed until the energy derivative was <0.001 kcal mol^{-1} $Å^{-1}$. Simulations were performed with zero, two, and eight fullerene molecules placed within the bilayer region.

RESULTS AND DISCUSSION

Solubilization of C_{60} in $CHCl_3$ and Entrapment Efficiency of Liposomes. Fullerenes were measured at 330 nm and the calibration curve was linear ($r^2 > 0.99$) in the range of 3.0−25.0 μg/mL in $CHCl_3$ ($A_{330} = -0.17338 + 0.0969$ [C_{60}], where [C_{60}] is the concentration of C_{60} in μg/mL). The amount of fullerene dissolved in the organic solvent was estimated to be 0.117 mg/mL, which is in broad agreement with the solubility values previously reported (solubility in $CHCl_3$ 0.16 mg/mL).[39]

The amount of C_{60} present in the membrane was calculated indirectly by measuring the nonencapsulated material. The C_{60} content in the liposomes was found to be 30% or 0.045 μmoles of the initial amount of C_{60} added to the liposomes.

Size Analysis and ζ-Potential Measurements. The DLS evaluation of plain and C_{60}-loaded liposomes in PBS pH 7.4 revealed a bimodal distribution for both plain and C_{60}-loaded liposomes (Figure 1). ILTs on the experimental data yield the distributions of the hydrodynamic radii that for liposomes exhibit two populations with average particle diameters of 146 ± 8 and 821 ± 35 nm, respectively. In a similar manner, C_{60}-loaded liposomes display two populations with average particle diameter of 183 ± 11 and 1288 ± 50 nm, accordingly. The significantly observed increase in C_{60}-loaded liposomes indicates the presence of C_{60} fullerenes in the lipid membrane (t test $p = 0.01$, $n = 3$). However, it should be stressed that Figure 1 illustrates the scattered intensity form of the ILT distributions. Taking into account the dependence of the scattered intensity on the sixth power of the particle size and the difference between the sizes of the two populations in each dispersion it is obvious that the population of large particles is much smaller than that of the small ones. In particular, we

dx.doi.org/10.1021/jp206221a | J. Phys. Chem. C 2012, 116, 3867−3874

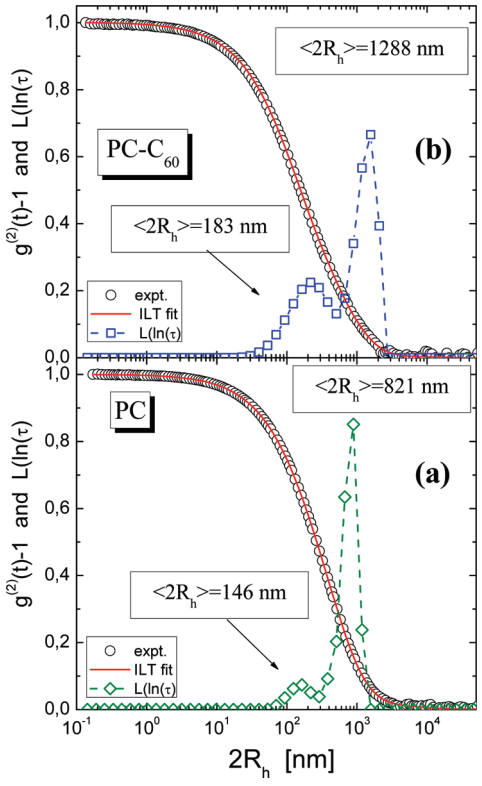

Figure 1. Inverse Laplace transform analysis of the experimental time correlation functions (eq 2) obtained by DLS for (a) plain and (b) C_{60}-loaded PC dispersions. Open circles: experimental data points. Solid lines: best fit curve obtained by ILT (eq 3). Open diamonds and squares: intensity distributions of the hydrodynamic diameters. Average magnitudes of the hydrodynamic diameters estimated by eq 4 are shown for each distribution.

estimate that the volume ratio of the small over the large particles is ca. 15 and 150 for PC and C_{60}-loaded PC dispersions, respectively. There was no significant difference in the ζ-potential values between the C_{60} liposomes (-1.52 ± 0.26 mV) and the plain ones (-1.03 ± 0.19 mV).

Miscibility Studies. The miscibility of C_{60} with PC liposomes was assessed by means of fluorescence spectroscopy. NR is a solvatochromic probe having a high affinity for lipid molecules.[40] The emission spectra of NR in plain and C_{60}-loaded liposomes are illustrated at Figure 2. Nonencapsulated NR, plain PC, and C_{60}-loaded liposomes were measured as controls under the same conditions. No emission spectra could be recorded for the controls, as illustrated in Figure 2. The emission of NR incorporated into both plain and C_{60}-loaded liposomes exhibits a maximum at $\lambda \approx 615$ nm. However the fluorescence intensity in plain liposomes is higher, implying that liposomes can accommodate higher numbers of NR molecules compared to the C_{60}-loaded PC liposomes. This conclusion is based on the fact that the same amount of NR was used in both plain and C_{60}-loaded liposomes and that NR when exposed to water experiences a dramatic decrease in its fluorescence emission. Another possible cause for the decrease in the fluorescence emission of NR in C_{60}-loaded liposomes could be the mere quenching of NR's emission by the presence of fullerenes. We investigated this by performing fluorescence measurements on NR solutions with increasing amounts of C_{60} (data not shown). It was found that C_{60}, even at concentrations of 30 μg/mL (similar to that found in the liposomes dispersion of Figure 2), decreases by only ~15% the fluorescence intensity of NR. This decrease is much lower than the 60% decrease observed in Figure 2. A third possibility has to do with the fact that if C_{60} and NR are both incorporated in the bilayer, then C_{60}'s relative concentration in the bilayer would be much higher than 30 μg/mL, and thus quenching might be possible.

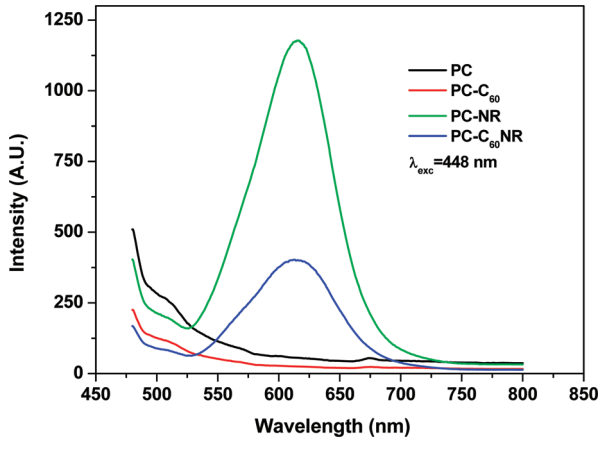

Figure 2. Fluorescence spectra of Nile Red (NR) in neat PC and PC-C_{60} liposomes, respectively. Data key presented in Figure inset.

NR can penetrate into the liposome bilayer, thus being less exposed to water. Therefore, according to the first explanation, the lower fluorescence emission of NR in C_{60}-loaded liposomes indicates the expulsion of NR when C_{60} molecules are present in the bilayer. The presence of C_{60} provides a lipid environment with lower incorporation capacity; therefore, the model compound is exposed to water.[41] In conclusion, having rejected the second possible cause for the fluorescence decrease and based on the other two possibilities as explained in the paragraph above, the experiment of Figure 2 suggests the incorporation of C_{60}s in the bilayer membrane.

Visualization Studies. The AFM studies revealed that the presence of fullerenes in the membranes induced considerable distortion in vesicle morphology (Figure 3 B, bottom image). The convex shape of both plain and C_{60}-loaded liposomes could be attributed to the tip compression force during imaging as well in some point to the coupling of liposome with the mica.

Plain liposomes (Figure 3A upper image) show smooth surface morphology, whereas the presence of fullerenes in the membranes results in polyhedral-like vesicles (Figure 3B, face indicated by a white arrow). This difference could also be observed in cross-section profile analysis (right images). On plain liposomes, the profile line appears as a smooth curve whereas on PC-C_{60}-loaded liposomes the profile line appears "crooked" when crossing from one particle "side" to the other. Moreover, "rod-like" structures (indicated by the blue arrow) might be attributed to the presence of C_{60} molecules to the membrane.

Liposome Stability Studies. The (%) latency of vesicle-encapsulated calcein is used as a measure of membrane integrity. From the results of these studies (Figure 4), it is clear that the PC-liposomes are stable because after 24 h of incubation, more than $68.57 \pm 2.29\%$ of the initially encapsulated calcein is retained in the vesicles, in accordance with previous studies.[42] On the contrary, when C_{60} were incorporated into the lipid bilayers, there is a pronounced effect on the stability of PC liposomes because a rapid decrease in the latency retention occurred within the first hour (from 75.27 ± 12.05 to $50.28 \pm 3.9\%$), followed by a leveling off up to 24 h

dx.doi.org/10.1021/jp206221a | J. Phys. Chem. C 2012, 116, 3867–3874

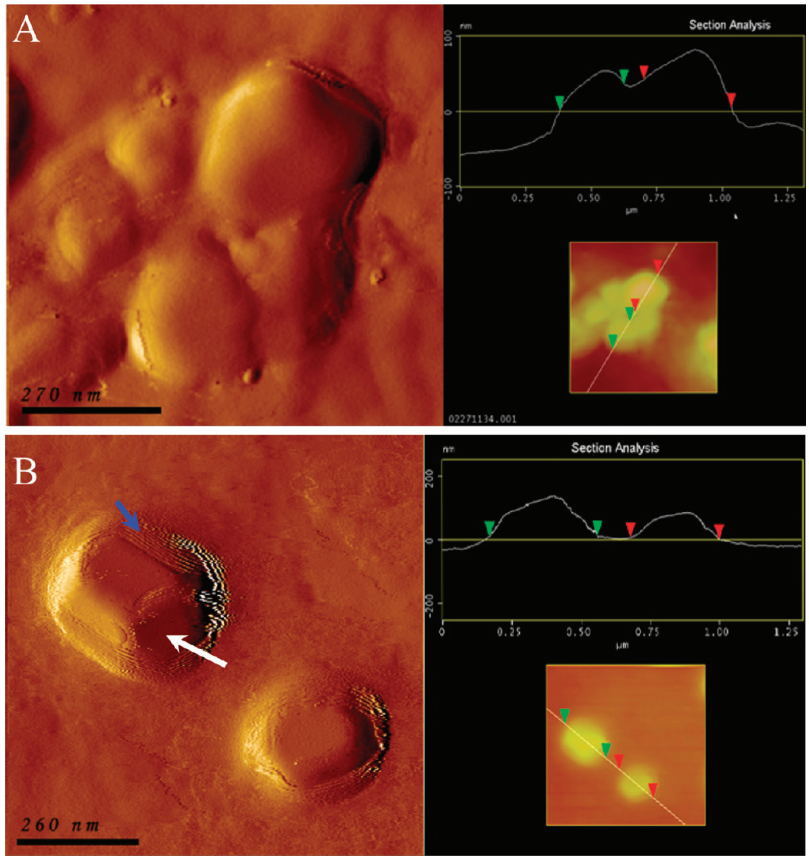

Figure 3. AFM images of (A) plain PC liposomes and (B) C_{60}-loaded PC liposomes. Bars are 270 and 260 nm, respectively.

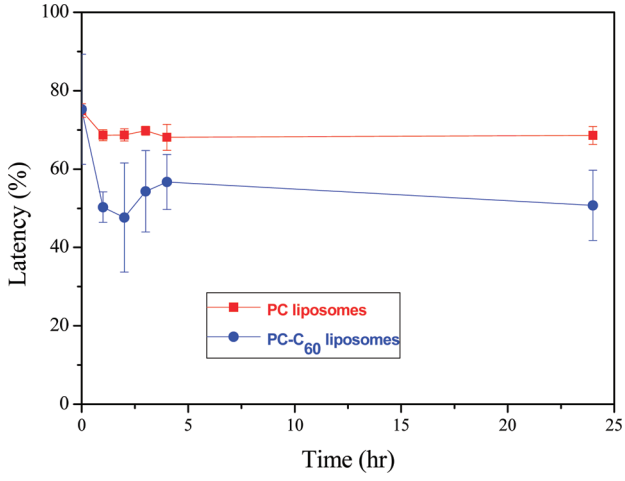

Figure 4. Calcein release (% of entrapped) from liposomes dispersed in PBS buffer pH 7.4 during incubation for a total period of 24 h. Data key presented in Figure inset (t test: $p < 0.05$).

(t-test; $p < 0.05$). These preliminary results imply that fullerenes destabilize the liposomal membrane over time. Previous studies have shown that C_{60} molecules form aggregates into the lipid membranes.[7] In a previous study, the presence of C_{60} in 1-palmitoyl-2-oleoylphosphatidylcholine (POPC) large unilamelar vesicles increased the stability of the liposomal membrane, as shown by carboxyflouroscein (CF) retention studies. These differences might be attributed to the different type of the lipid and the temperature used for monitoring the release of CF.[43] Very recently, in an experimental study Zupanc et al. showed that C_{60} water suspension causes changes of the average mean curvature of the lipid membrane, leading to the rupture of POPC vesicles.[44]

Proliferative Studies. The effect of freshly prepared C_{60}-loaded liposomes, plain liposomes, and free C_{60} on 3T3 cell activity was assessed using the MTT assay. It can be seen that C_{60}-loaded liposomes did not show any detrimental effect on the 3T3 activity after 24 h of incubation (t test: $p < 0.001$) (Figure 5 A). At least 50% of the initial amount of incorporated fullerene is still retained in the formulation. Plain PC liposomes did not affect the cell viability, as expected. Free fullerenes significantly affected the cell activity at concentrations of either 100 μg/mL or equal to that contained in 400 μg/mL, as shown in Figure 5B. The results suggest that the cytotoxic effect of fullerene was reduced significantly after its incorporation into the liposomal bilayer after 24 h of incubation with the rodent fibroblasts, at which fullerene toxicity depends on its derivatization,[45,46] the solvent it is dispersed in, and its solubility,[47,48] concentration, size, and route of exposure.[47] It has been reported that the action of fullerene can be ambiguous as it is dose-dependent. Therefore, fullerene can be beneficial at low dose as a scavenger of reactive oxygen species and free radicals, thus yielding an antitumor effect due to phototoxic reactions. C_{60} can be harmful at higher doses as it has been shown to cause lipid peroxidation of cell membrane lipids, radical formation, inflammation, and cancer.

The most prominent mechanism of fullerene cytotoxicity is the production of reactive oxygen species and cell membrane lipid peroxidation and necrotic cell death. However, Spohn

dx.doi.org/10.1021/jp206221a | J. Phys. Chem. C 2012, 116, 3867–3874

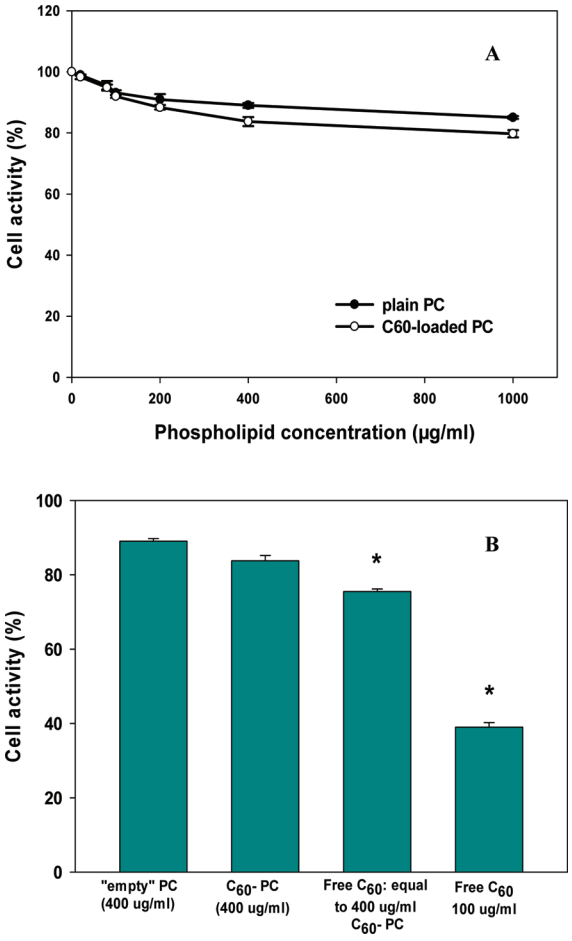

Figure 5. (A) 3T3 cell proliferation after 24 h of incubation with either plain PC liposomes or C_{60}-loaded liposomes. (B) Comparison of cell proliferation in the presence of the "empty" PC, C_{60}-loaded PC liposomes, free fullerenes (C_{60}) at concentration equal to that contained in 400 μg/mL, and free C_{60} after 24 h of incubation with 3T3 cells (t test: $p < 0.001$).

et al.[47] showed that fullerene was not toxic toward the epithelial cell line A549 after 6 days of incubation. On the contrary, fullerene and its derivatives showed a profound difference in cytotoxicity on various cell lines, as was shown by Sayes et al.,[49,50] who reported that LC50 varies from 2 to 50 μg/L for neuronal human astrocytes and human liver carcinoma cells, respectively, after 48 h of incubation. Our results agree with those of Sayes et al.,[49] but the effect of fullerene on cell viability is in the ppm and not the ppb range as the authors have reported. However, there are no data reported elsewhere on the fullerene toxicity on 3T3 cells.

Molecular Simulation Studies. The structure of the lipid and the carboanceous material is shown in Figure 6. The optimized lipid bilayer in the absence of C_{60} is illustrated in Figure 7A. An overview of the lipid bilayer viewed from the top with the water molecules removed (for clarity) is shown in Figure 7 B. At low concentrations of C_{60} (2 per simulation box), the carbonaceous material is incorporated into the bilayer toward the middle of the layer. This observation is inconsistent with long MD simulations perfomed on C_{60} within a phosphatidylcholine bilayer, supporting the validitiy of our approach.[20] When higher concentrations of fullerenes were present in the liposomal bilayer, as illustrated in Figure 9A, the

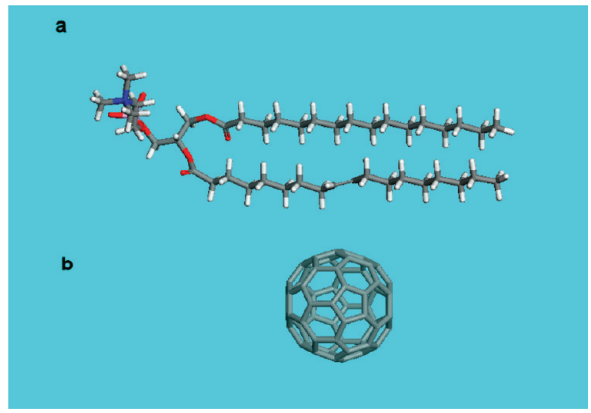

Figure 6. (a) Structure of phosphatidycholine and (b) fullerene.

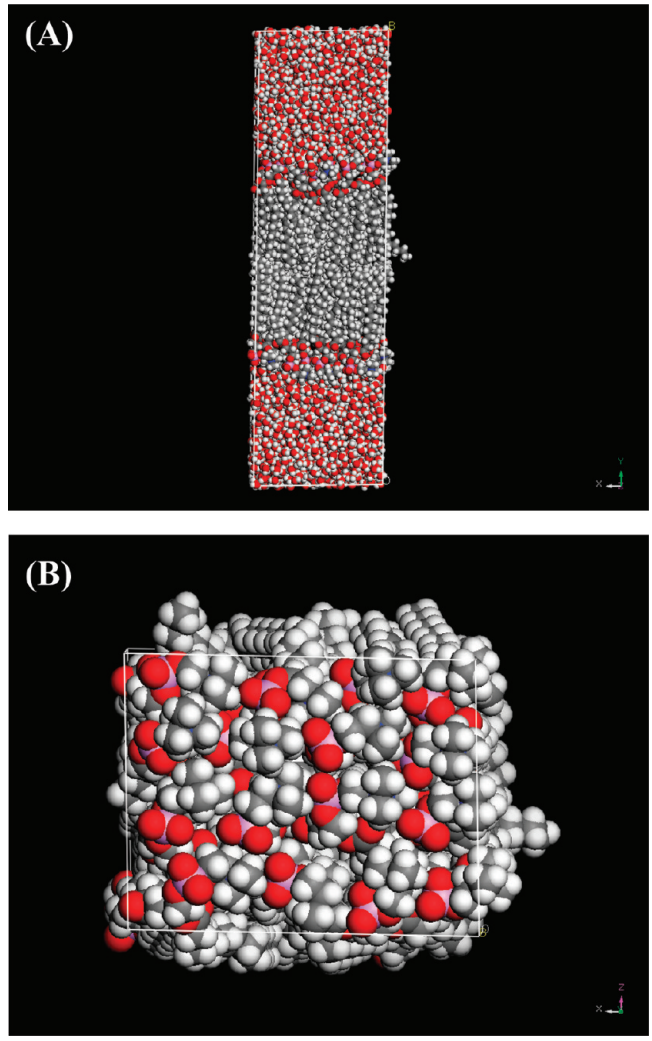

Figure 7. (A) Optimized lipid bilayer without C_{60} molecules. (B) Optimized phospholipid bilayer viewed from top (water molecules removed for clarity).

C_{60} molecules are much more readily seen, suggesting that significant disruption to the surface of the bilayer has occurred.

Figure 8 shows how the hydrophobic tails of the PC wrap themselves around the C_{60} molecule to maximize the van der Waals interactions. At this low concentration of C_{60} molecules, no disruption of the surface of the bilayer is observed and the

dx.doi.org/10.1021/jp206221a | J. Phys. Chem. C 2012, 116, 3867–3874

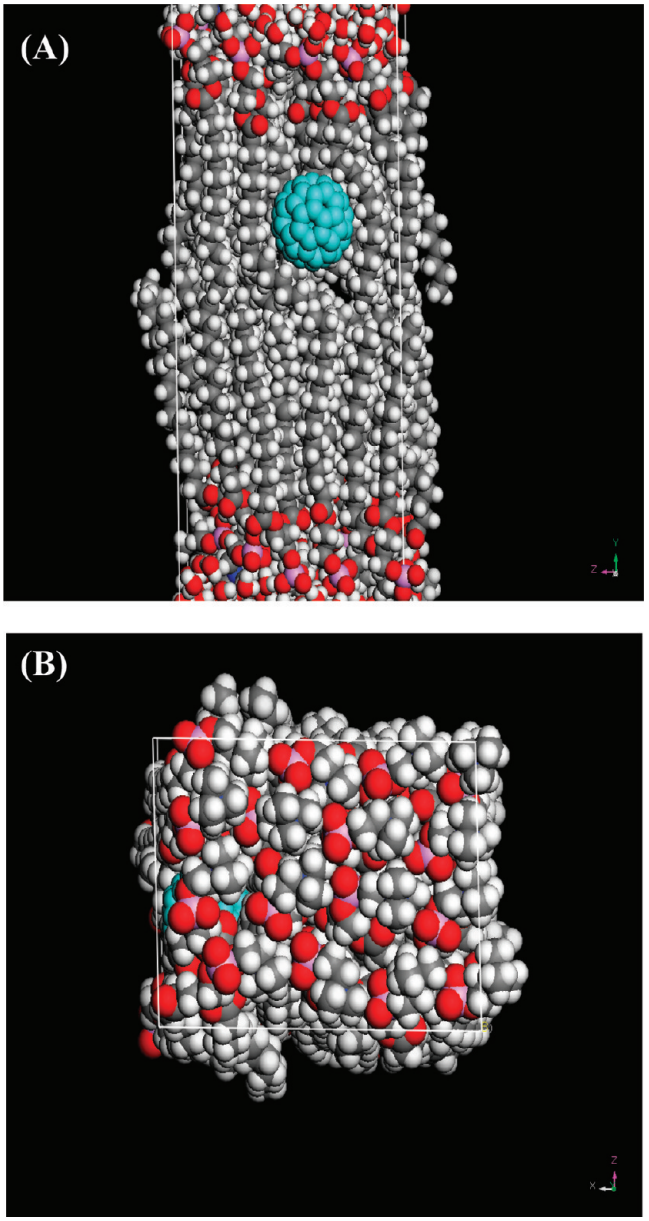

Figure 8. (A) Optimized lipid bilayer with two C_{60} molecules per simulation box. The one C_{60} molecule visible in this orientation is shown in light blue. (B) Optimized phospholipid bilayer viewed from the top (water molecules removed for clarity).

surface viewed from above (Figure 8B) appears similar to that shown in Figure 7B, with the C_{60} molecule largely shielded from view. The hydrophobic tails of the phospholipids again "mold" themselves around fullerene molecules, but at higher concentrations adjacent fullerenes are displaced higher up the bilayer toward the hydrophilic head of the phospholipid molecules (Figure 9B), thus disrupting the surface. This effect is also reflected in the calculated size of the surface area for each of the three simulations. At low concentration of fullerene (2 molecules per simulation box) and with no fullerene present, the surface area remains largely unchanged, with values of 840 and 835 $Å^2$ obtained, respectively.

However, at the higher concentration of fullerene (eight molecules per simulation box), the surface area increases significantly to 1003 $Å^2$, reinforcing the suggestion that low

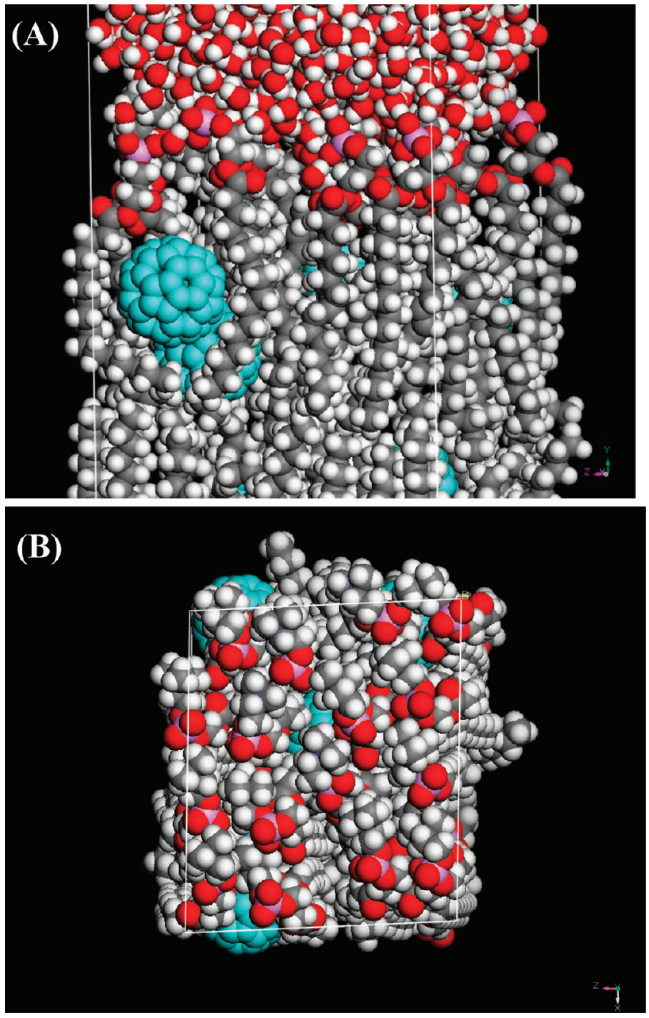

Figure 9. (A) Optimized lipid bilayer with eight C_{60} molecules per simulation box. The C_{60} molecules visible in this orientation are shown in light blue. (B) Optimized phospholipid bilayer viewed from the top (water molecules removed for clarity).

quantities of fullerene have little effect on the surface of the bilayer but that high concentrations can disrupt it substantially.

At both concentrations, incorporation of the fullerene into the bilayer results in a favorable binding energy (−261 and −289 kcal mol^{-1} at low and high concentrations, respectively), although we note that the binding energy per C_{60} molecule is higher at low concentration (−131 kcal mol^{-1}) than at high concentration (−36 kcal mol^{-1}). The theoretical observations in this work are supported by our experimental measurements that show that the lipid membrane becomes "leaky" at high loading of C_{60} and provide a clear rationale for this observation.

■ CONCLUSIONS

Toward the understanding of the interactions between lipid bilayers with unmodified C_{60}, a combination of experimental and theoretical techniques have been employed to assess the stability and the integrity of the lipid membrane.

The fluorescence spectroscopy studies have confirmed the miscibility of the fullerenes with the lipid bilayer. AFM imaging has shown that the presence of fullerenes in the membrane induce structural changes within the produced vesicles in PBS, the biological relevant medium used in this study. Integrity studies revealed that the incorporation of C_{60} molecules can

dx.doi.org/10.1021/jp206221a | J. Phys. Chem. C 2012, 116, 3867−3874

induce disruption of the membrane based on the retention values of the hydrophilic marker calcein. The fullerene cytotoxic effect was reduced significantly after its incorporation into the liposomal bilayer after 24 h of incubation with the rodent fibroblasts mitigating the risk for their use to biomedical applications. Finally, the experimental data are corroborated by the theoretical calculations where high concentrations of fullerenes to the membrane induce disruption to the surface, which is not the case for low concentration of fullerene as the membrane remains intact.

On the basis of the data presented in the current study, it can be anticipated that the amount of C_{60} present in the membrane is directly linked to its integrity; therefore, studies varying the concentration of fullerenes up to the saturation of the membrane and the type of liposomes in terms of size and lamellarity can offer insight into the stability of these dispersions and therefore lay the frame for future work.

AUTHOR INFORMATION

Corresponding Author

*E-mail: nbouro@upatras.gr. Tel: +30 2610 997874. Fax: +30 2610 969368.

Present Addresses

▽Division of Biopharmaceutics and Pharmacokinetics, Faculty of Pharmacy, Viikinkaari 5 E (P.O. Box 56), 00014 University of Helsinki, Finland.

○Aristotle University of Thessaloniki, School of Pharmacy, Department of Pharmaceutical Technology, GR-54124 Thessaloniki, Greece.

Notes

The authors declare no competing financial interest.

ACKNOWLEDGMENTS

We acknowledge the technical assistance provided by Dr. E. Karoutsos for the AFM measurements.

REFERENCES

(1) Lens, M.; Medenica, L.; Citernesi, U. *Biotechnol. Appl. Biochem.* **2008**, *51*, 135.

(2) Zakharian, T. Y.; Seryshev, A.; Sitharaman, B.; Gilbert, B. E.; Knight, V.; Wilson, L. J. *J. Am. Chem. Soc.* **2005**, *127*, 12508.

(3) Shu, C. Y.; Ma, X. Y.; Zhang, J. F.; Corwin, F. D.; Sim, J. H.; Zhang, E. Y.; Dorn, H. C.; Gibson, H. W.; Fatouros, P. P.; Wang, C. R.; Fang, X. H. *Bioconjugate Chem.* **2008**, *19*, 651.

(4) Markovic, Z.; Trajkovic, V. *Biomaterials* **2008**, *29*, 3561.

(5) Cagle, D. W.; Kennel, S. J.; Mirzadeh, S.; Alford, J. M.; Wilson, L. *Proc. Nat. Acad. Sci. U.S.A.* **1999**, *96*, 5282.

(6) Akiyama, M.; Ikeda, A.; Shintani, T.; Doi, Y.; Kikuchi, J.; Ogawa, T.; Yogo, K.; Takeya, T.; Yamamoto, N. *Org. Biomol. Chem.* **2008**, *26*, 1015.

(7) Hungerbuhler, H.; Guldi, D. M.; Asmus, K. D. *J. Am. Chem. Soc.* **1993**, *115*, 3386.

(8) Levi, N.; Hantgan, R. R.; Lively, M. O.; Carroll, D. L.; Prasad, G. L. *J. Nanobiotechnol.* **2006**, *4*, 14.

(9) Li, W. Z.; Qian, K. X.; Huang, W. D.; Zhang, X. X.; Chen, W. X. *Chin. Phys. Lett.* **1994**, *11*, 207.

(10) Kallinteri, P.; Antimisiaris, S. G.; Fatouros, D. G. Chapter 5.3 Liposomes and Drug Delivery. In *Pharmaceutical Manufacturing Handbook: Production and Processes, Special New Dosage Forms*; Gad, S. C., Ed.; Wiley and Sons: Hoboken, NJ, 2008; pp 443−534.

(11) Bensasson, R. V.; Bienvenue, E.; Dellinger, M.; Leach, S.; Seta, V. *J. Phys. Chem.* **1994**, *98*, 3942.

(12) Janot, J. M.; Bienvenüe, E.; Seta, P.; Bensasson, R. V.; Tomé, A. C.; Enes, R. F.; Cavaleiro, J. A. S.; Leach, S.; Camps, X.; Hirsch, A. *J. Chem. Soc., Perkin Trans.* **2000**, *2*, 301.

(13) Braun, M.; Hirsch, A. *Carbon* **2000**, *38*, 1565.

(14) Ikeda, A.; Sato, T.; Kitamura, K.; Nishiguchi, K.; Sasaki, Y.; Kikuchi, J.; Ogawa, T.; Yogo, K.; Takeya, T. *Org. Biomol. Chem.* **2005**, *3*, 2907.

(15) Ikeda, A.; Doi, Y.; Nishiguchi, K.; Kitamura, K.; Hashizume, M.; Kikuchi, J.; Ogawa, T.; Yogo, K.; Takeya, T. *Org. Biomol. Chem.* **2007**, *5*, 1158.

(16) Jeng, U.; Lin, T. L.; Shin, K.; Hsu, C. H.; Lee, H. Y.; Wu, M. H.; Chi, Z. A.; Shih, M. C.; Chiang, L. Y. *Phys. B* **2003**, *336*, 204.

(17) Bensasson, R. V.; Garaud, J. L.; Leach, S.; Miquel, G.; Seta, P. *Chem. Phys. Lett.* **1993**, *210*, 141.

(18) Hetzer, M.; Bayerl, S. Dr.; Camps, X.; Vostrowsky, O.; Hirsch, A.; Bayerl, T. M. *Adv. Mater.* **1997**, *9*, 913.

(19) Qiao, R.; Roberts, A. P.; Mount, A. S.; Klaine, S. J.; Ke, P. C. *Nano Lett.* **2007**, *7*, 614.

(20) Li, L.; Davande, H.; Bedrov, D.; Smith, G. D. *J. Phys. Chem. B* **2007**, *111*, 4067.

(21) Bedrov, D.; Smith, G. D.; Davande, H.; Li, L. J. *Phys. Chem. B* **2008**, *112*, 2078.

(22) Wong-Ekkabut, J.; Baoukina, S.; Triampo, W.; Tang, I. M.; Tieleman, D. P.; Monticelli, L. *Nat. Nanotechnol.* **2008**, *6*, 363.

(23) Katsamenis, O. L.; Bouropoulos, N.; Fatouros, D. G. *J. Biomed. Nanotechnol.* **2009**, *5*, 416.

(24) Chen, Y.; Bothun, G. D. *Langmuir* **2009**, *25*, 4875.

(25) Stewart, J. C. M. *Anal. Biochem.* **1980**, *104*, 10.

(26) Berne, B. J.; Pecora, R. *Dynamic Light Scattering*; Wiley: New York, 1976.

(27) Provencher, S. W. *Comput. Phys. Commun.* **1982**, *27*, 213.

(28) Kirby, C.; Clarke, J.; Gregoriadis, G. *Biochem. J.* **1980**, *186*, 591.

(29) Fatouros, D. G.; Antimisiaris, S. G. *J. Colloid Interface Sci.* **2002**, *251*, 271.

(30) Mosmann, T. *J. Immunol. Methods* **1983**, *65*, 55.

(31) *Materials Studio*, version 4.1; Accelrys: San Diego, CA, 2007.

(32) Maple, J. R.; Hwang, M. J.; Stockfish, T. P.; Dinur, U.; Waldman, M.; Ewig, C. S.; Hagler, A. T. *J. Comput. Chem.* **1994**, *15*, 162.

(33) Marcorin, G. L.; Da Ros, T.; Castellano, S.; Stefancich, G.; Bonin, I.; Miertus, S.; Prato, M. *Org. Lett.* **2000**, *14*, 3955.

(34) Xiang, T. X.; Anderson, B. D. *Biophys. J.* **2002**, *82*, 2052.

(35) Felder-Flesch, D.; Rupnicki, L.; Bourgogne, C.; Donnio, B.; Guillon, D. *J. Mater. Chem.* **2006**, *16*, 304.

(36) Stouch, T. R. *Mol. Simul.* **1993**, *10*, 335.

(37) Alper, H. E.; Bassolino-Klimas, D; T. R. Stouch, T. R. *J. Chem. Phys.* **1993**, *98*, 9798.

(38) Alper, H. E.; Bassolino-Klimas, D; Stouch, T. R. *J. Chem. Phys.* **1993**, *99*, 5547.

(39) Ruoff, R. S.; Doris, S.; Tse, D. S.; Malhotra, R.; Lorents, D. C. *J. Phys. Chem.* **1993**, *97*, 3379.

(40) Greenspan, P.; Fowler, S. D. *J. Lipid Res.* **1985**, *26*, 781.

(41) Feitosa, E.; Alves, F. R.; Niemiec, A.; Real Oliveira, M. E. C. D.; Castanheira, E. M. S.; Baptista, A. F. L. *Langmuir* **2006**, *22*, 3579.

(42) Hatzi, P.; Mourtas, S.; Klepetsanis, P. G.; Antimisiaris, S. *Int. J. Pharm.* **2007**, *333*, 167.

(43) De Maria, P.; Fontana, A; Gasbarri, C.; Velluto, D. *Soft Matter.* **2006**, *2*, 595.

(44) Zupanc, J.; Drobne, D.; Drasler, B.; Valant, J.; Iglic, A.; Kralj-Iglic, V.; Makovec, D.; Rappolt, M.; Sartori, B.; Kogej, K. *Carbon* **2012**, *50*, 1170.

(45) Nielsen, G. D.; Roursgaard, M.; Jensen, K. A.; Poulsen, S. S.; Larsen, S. T. *Basic Clin. Pharmacol. Toxicol.* **2008**, *103*, 197.

(46) Zhang, W. L.; Yang, J.; Barron, A. R.; Monteiro-Riviere, N. A. *Toxicol. Lett.* **2009**, *191*, 149.

(47) Spohn, P.; Hirsch, C.; Hasler, F.; Bruinink, A.; Krug, H. F.; Wick, P. *Environ. Pollut.* **2009**, *157*, 1134.

(48) Rajagopalan, P.; Wudl, F.; Schinazi, R. F.; Boudinot, F. D. *Antimicrob. Agents Chemother.* **1996**, *40*, 2262.

(49) Sayes, M. C.; Gobin, A. M.; Ausman, K. D.; Mendez, J.; West, J. L.; Colvin, V. L. *Biomaterials* **2005**, *26*, 7587.

(50) Sayes, C. M.; Fortner, J. D.; Guo, W.; Lyon, D.; Boyd, A. M.; Ausman, K. D.; Tao, Y. J.; Sitharaman, B.; Wilson, L. J.; Hughes, J. B.; West, J. L.; Colvin, V. L. *Nano Lett.* **2004**, *4*, 1881.